AN ANALYSIS OF SmBa 0.5Sr UDC 539 0.5CO2O5+δ DOUBLE PEROVSKITE OXIDE FOR INTERMEDIATE–EMPERATURE SOLID OXIDE FUEL CELLS

By Ratna kartikasari

WORD COUNT 7130

TIME SUBMITTED 05-MAY-2021 09:54AM

PAPER ID 71800435

MATERIALS SCIENCES

UDC 539
DOI: 10.15587/1729-4061.2021.226342

AN ANALYSIS OF $SmBa_{0.5}Sr_{0.5}CO_2O_{5+\delta}$ DOUBLE PEROVSKITE OXIDE FOR INTERMEDIATE–TEMPERATURE SOLID OXIDE FUEL CELLS

Adi Subardi
Doctor of Materials Science and Engineering, Assistance Professor*
E-mail: subardi@itny.ac.id
Iwan Susanto
Doctor of Materials Science and Engineering, Assistance Professor
Department of Mechanical Engineering
Politeknik Negeri Jakarta
Jl. Prof. DR. G.A. Siwabessy, Kukusan, Kecamatan Beji, Kota Depok, Jawa Barat, Indonesia, 16424
Ratna Kartikasari
Doctor of Mechanical Engineering, Associate Professor*
Tugino Tugino
Master of Electrical Engineering, Associate Professor
Department of Electrical Engineering**
Hasta Kuntara
Master of Mechanical Engineering, Assistance Professor*
Andy Erwin Wijaya
Doctor of Mining Engineering, Assistance Professor
Department of Mining Engineering**
Muhamad Jalu Purnomo
PhD, Assistance Professor
Departement of Aeronautics
Institut Teknologi Dirgantara Adisutjipto
Jl. Amarta Blok R, Karang Janbe, Banguntapan, Kec. Banguntapan, Bantul, Daerah Istimewa, Yogyakarta, Indonesia, 55198
Ade Indra
PhD, Associate Professor***
Hendriwan Fahmi
Master of Mechanical Engineering, Associate Professor***
Yen-Pei Fu
Doctor of Materials, Professor
Department of Materials Science and Engineering
National Dong Hwa University
Shoufeng Township, Hualien, Taiwan, 97401
*Department of Mechanical Engineering**
**Institut Teknologi Nasional Yogyakarta
Jl. Babarsari, Caturtunggal, Depok, Sleman, Daerah Istimewa Yogyakarta, Indonesia, 55281
***Department of Mechanical Engineering
Institut Teknologi Padang (ITP)
Jl. Gajah Mada Jl. Kandis Raya, Kp. Olo, Kec. Nanggalo, Kota Padang, West Sumatera Barat, Indonesia, 25173

The main obstacle to solid oxide fuel cells (SOFCs) implementation is the high operating temperature in the range of 800–1,000 °C so that it has an impact on high costs. SOFCs work at high temperatures causing rapid breakdown between layers (anode, electrolyte, and cathode) because they have different thermal expansion. The study focused on reducing the operating temperature in the medium temperature range. $SmBa_{0.5}Sr_{0.5}Co_2O_{5+\delta}$ (SBSC) oxide was studied as a cathode material for IT-SOFCs based on $Ce_{0.8}Sm_{0.2}O_{1.9}$ (SDC) electrolyte. The SBSC powder was prepared using the solid-state reaction method with repeated ball-milling and calcining. Alumina grinding balls are used because they have a high hardness to crush and smooth the powder of SOFC material. The specimens were then tested as cathode material for SOFC at intermediate temperature (600–800 °C) using X-ray powder diffraction (XRD), thermogravimetric analysis (TGA), electrochemical, and scanning electron microscopy (SEM) tests. The X-ray powder diffraction (XRD) pattern of SBSC powder can be indexed to a tetragonal space group (P4/mmm). The overall change in mass of the SBSC powder is 8 % at a temperature range of 125–800 °C. A sample of SBSC powder showed a high oxygen content (5+δ) that reached 5.92 and 5.41 at temperatures of 200 °C and 800 °C, respectively. High diffusion levels and increased surface activity of oxygen reduction reactions (ORRs) can be affected by high oxygen content (5+δ). The polarization resistance (Rp) of samples sintered at 1000 °C is 4.02 Ωcm^2 at 600 °C, 1.04 Ωcm^2 at 700 °C, and 0.42 Ωcm^2 at 800 °C. The power density of the SBSC cathode is 336.1, 387.3, and 357.4 mW/cm^2 at temperatures of 625 °C, 650 °C, and 675 °C, respectively. The SBSC demonstrates as a prospective cathode material for IT-SOFC.

Keywords: solid oxide fuel cell, thermal properties, oxygen content, electrochemical properties, cell performance

Received date 16.12.2020
Accepted date
Published date

***How to Cite**: Subardi, A., Susanto, I., Kartikasari, R., Tugino, T., Kuntara, H., Wijaya, A. E., Purnomo, M. J., Indra, A., Fahmi, H., Fu, Y.-P. (2021). Analysis of SmBa0.5Sr0.5Co2O5+δ double perovskite oxide for intermediate–temperature solid oxide fuel cells. Eastern-European Journal of Enterprise Technologies, 2 (6 (110)), 6–14. doi: https://doi.org/10.15587/1729-4061.2021.226342*

1. Introduction

Limited fossil fuels and global warming are increasingly threatening human survival and have been serious global issues for decades. New power plants using fuel sources such as solid oxide fuel cells (SOFCs) have attracted much attention around the world, and the technology is expected to reduce obstacles in the supply of electricity in the future. The advantage of SOFCs compared with other types of fuel cells is that they are a more efficient and flexible fuel source.

SOFCs also offer low pollutant emissions because the final stage of their usage only produces vapor or hot water [1–3]. The schematic diagram exhibiting the basic operation of SOFC is shown in Fig. 1, *a*. At the cathode side, the oxygen reduction reaction occurs by accepting electrons from the external circuit. The reactions can be written below:

$$O_2+4e^-\rightarrow 2O^{2-}. \quad (1)$$

The produced oxide ions (O^{2-}) pass through the electrolyte to the anode side and combine with the protons produced by the oxidation of hydrogen or other fuels to produce water. The reactions can be written as follows:

$$2H_2+2O^{2-}\rightarrow 2H_2O+4e^-. \quad (2)$$

Overall reaction,

$$2H_2+O_2\rightarrow 2H_2O. \quad (3)$$

This reaction occurs at the three-phase boundary (TPB) [4]. The TPB is the interfacial area among electrode, electrolyte, and gaseous fuel where the overall reaction occurs (Fig. 1, *b*). The electrons flowing from the anode to the cathode produce electrical work in the "Load".

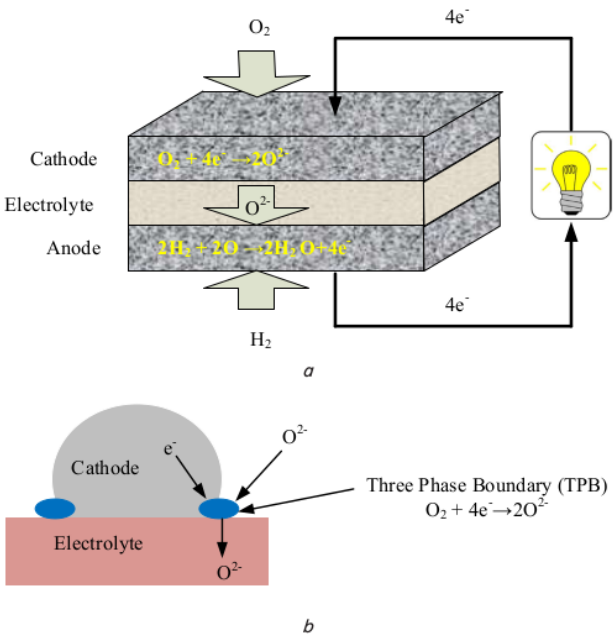

Fig. 1. Schematic diagram: *a* — SOFC operation; *b* — three-phase boundary (TPB)

Through the process, chemical energy is directly converted to electrical energy. To increase the active area where the oxygen reduction reaction (cathode) or hydrogen oxidation reaction (anode) occurs, a porous electrode structure is employed. Meanwhile, the dense electrolyte provides a physical barrier to prevent the direct mixing of fuel and air.

2. Literature review and problem statement

In general, traditional SOFCs operate at high temperatures, which causes several problems including high production costs, mismatches in thermal expansion between the fuel cell components, and chemical compatibility. Therefore, current research is focused on SOFCs that can operate at lower temperatures (400–800 °C) and aims to reduce production costs and achieve a long working lifetime (40.000 h) [5–7]. Lower operating temperatures cause the catalytic activity of the electrodes to decrease significantly, and the cathode is a limiting factor for the overall fuel cell performance. Therefore, the focus is being directed toward maintaining stability in the cathode material and increasing the high electrochemical performance of IT-SOFCs. In other words, a vital result of the research into fuel cell performance is the discovery that the cathode polarization can be eliminated [8]. However, the application of SOFC is widely constrained due to the impact of low catalytic activity on the oxygen reduction reactions (ORRs) at the cathode. Mixed ionic-electronic conductor cathodes (MIECs) are successful in increasing the active ORR zone from the three-phase boundary to the cathode-gas interface site, which will reduce cathodic resistance [8, 9]. The ORR site of MIECs works on the TPB (the electrolytes, cathodes, and gas phases) and at the two-phase boundary between the gas phase and the cathode [10].

Recently, among the various MIECs oxides, cobalt-containing perovskite oxides such as Sm-$Ba_{0.6}Sr_{0.4}Co_2O_{5+\delta}$ [11], $PrBa_{0.5}Sr_{0.5}Co_{2x}Fe_xO_{5+\delta}$ [12], $NdBa_{1-x}Sr_xCo_2O_{5+\delta}$ [13], $YBa_{0.6}Sr_{0.4}Co_2O_{5+\delta}$ [14], and $GdBa_{0.5}Sr_{0.5}Co_{2-x}Fe_xO_{5+\delta}$ [15] have attracted strong interest due to their electrocatalytic activity performance for the ORR. Also, the investigation has been conducted for layered perovskites with the chemical formula $LnBaCo_2O_{5+\delta}$ (Ln-selected lanthanides) [16–23]. Several research groups also have investigated the electrochemical properties of a new type of MIEC oxide, cation ordered Ln-$BaCo_2O_{5+\delta}$ (Ln=La, Pr, Sm, Gd, Y), as a potential cathode material for IT-SOFCs. Cobalt in cathodes is beneficial for the activation of oxygen reduction and thus provides a lower activation polarization loss. Cobalt-based cathodes, however, have high thermal expansion coefficients (TECs) because of the low-spin to the high-spin transition of Co. The incompatibility in thermal expansion can cause thermal stress in SOFCs and thus result in poor long-term thermal stability [13]. Therefore, it is important to improve the thermal expansion compatibility between the cathodes and the electrolytes. Zhou *et al.* [24] have declared that $LnBaCo_2O_{5+\delta}$ cathodes with an intermediate lanthanide-ion radius, such as Sm^{3+}, may provide a compromise between the values of the catalytic activity and thermal expansion coefficients. Recent reports exhibit when A′ site is partially substituted by Sr, it could potentially improve the conductivity of double perovskite oxides where Sr-doped oxide $YBa_{0.5}Sr_{0.5}Co_2O_{5+\delta}$ demonstrated excellent conductivity values (about 32 times higher than that of the Sr-free sample). Moreover, the Sr-doped layered perovskite oxide system $LnBa_{0.5}Sr_{0.5}Co_2O_{5+x}$ (Ln=Pr, Sm, and Gd), which showed a lower polarization resistance based on doped ceria electrolyte [25]. However, observations of SOFC performance in the range of 625, 650, and 675 °C

have not been experimentally investigated. From the research reported above, some of the obstacles that SOFC faced were high working temperatures and high thermal expansion differences in SOFC components. Efforts were made to overcome this problem, the use of SBSC material as a cathode is expected to reduce the working temperature of SOFC so that the compatibility of SOFC components meets the requirements. In this work, SBSC oxide is synthesized, and aspects of its structural characteristics, thermal and electrochemical performance, power density, and microstructure are investigated. The SBSC oxygen reduction mechanism is also observed under various oxygen partial pressures (OPPs).

3. The aim and objectives of the study

The aim of this study was to analyze the performance of double perovskite oxides used in intermediate-temperature solid oxide fuel cells.

To achieve this aim, the following objectives are accomplished:

– to modify the structure of SBSC cathode by the solid-state reaction method;

– to investigate the polarization resistance (R_p) of SBSC cathode and the maximum power density obtained in the single SOFC;

– to test the performance of SBSC cathodes at intermediate operating temperatures.

4. Materials and methods for preparing and testing specimens

Fig. 2 shows the procedure of preparation for the single cell specimen, which consists of three SOFC elements, namely anode, electrolyte and cathode materials. The synthesis methods for the cathodes and electrolytes are described in previously published papers [11, 26]. The SBSC cathode powder was prepared using a solid-state reaction technique. The stoichiometric amounts of cathode material (Sm_2O_3, $BaCO_3$, $SrCO_3$, and CoO) were ball-milled in ethanol for 12 h. The slurry was then heated at a temperature of 1,000 °C in the air for 6 h. The $Ce_{0.8}Sm_{0.2}O$ (SDC) powder was synthesized using the coprecipitation technique using the precursor materials $Ce(NO_3)_3.6H_2O$ and $Sm(NO_3)_3.6H_2O$. A stoichiometric ratio was applied, distilled water was then used to dissolve the starting material before being added to the ammonia solution.

The pH value ranging from 9.5 to 10 is applied to the mixed solution. The precipitate was washed three times after it was filtered using distilled water and ethanol. In the next process, the co-precipitation powder was heated at 600 °C and held in the air for 2 h. For a binding agent, a small amount of polyvinyl alcohol (PVA) with a purity grade of 96 % was mixed into the SDC powder and then pelletized to dimensions of 1.5 cm in diameter and 0.1 cm in thickness using uniaxial pressure applied at 1,000 kg f/cm^2. The disk-shaped sample was heated at 1,500 °C and held for 5 h, followed by cooling to room temperature [26]. The procedure stages of fabricating a single cell specimen are presented in Fig. 2. The structure of the SBSC cathode powder was observed by XRD using Rigaku D/MAX-2500V, the radiation source of Cu Kα (1.5418 Å), and a scanning range of 10°–80°. To explain the lattice parameter and powder pattern for the sample, we used the GSAS program to perform a Rietveld refinement. The SBSC cathode microstructure (top view) and the cross-sectional image of the symmetrical cell were investigated by SEM (Hitachi 3400N). The TG/DTA 6300 was used to analyze the thermo-gravimetric behavior of SBSC cathodes in the air (100 cm^3/min). The oxygen content was calculated using the following formula:

$$\delta = \frac{M_s \Delta m}{M_o m}. \quad (4)$$

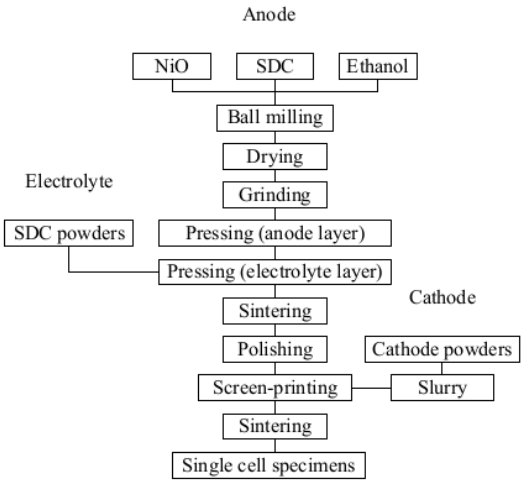

Fig. 2. Procedure of preparation for single-cell specimens

The abbreviations/symbols in the formula are explained as follows, the specimen molar mass (M_s), the specimen mass in the air at room temperature (m), and the molar mass of oxygen (M_o) [27]. The cathode paste of SBSC involves cathode powder, the binding agent, a plasticizer, and a solvent, all of which were conducted by ball-mill processes. Screen printing technique was used to prepare a half cell sample of SBSC|SDC|SBSC. The manufacturing details of the half-cell sample are discussed in the earlier paper. The symmetrical cell testing was carried out under air at temperatures ranging from 600 °C to 800 °C in a furnace. The AC impedance measurement was performed using the VoltaLab PGZ301 potentiostat with a frequency applied range from 100 kHz to 0.1 Hz with 10 mV AC signal amplitude. The EIS fitting analysis was performed with the Z-view software [24]. The digital source meter (Keithley 2420) was used to collect voltage (V) – current (I) from a single cell in the temperature range between 625 °C and 675 °C. Button cells were measured with humidified hydrogen (3 vol % H_2O) as the fuel and air as the oxidant. The configuration of the single-cell sample was Ni-SDC|SDC|SBSC with a 1.3 cm diameter. In the preceding paper [28], the detailed stages for preparing a single cell are given.

5. Results of SBSC Performance Test

5. 1. Crystal Structure

The crystal structure and phase composition of the SBSC powder were observed using X-ray diffraction (XRD). From the GSAS software analysis, characteristic XRD peaks were

detected as double perovskite oxide. The peaks caused by impurities are not detected in the structure of SBSC, which indicates a well-prepared sample. Meanwhile, the lattice parameters are obtained: a=3.861 Å, b=3.861 Å, c=7.617 Å, and v=113.56 Å^3, with reliability factors of R_{wp}=0.41 and R_p=0.23. In this structure, Sm atoms are in position 1a, Sr, and Ba atoms are randomly distributed at position 1b. The cell parameters regarding the SBSC cathode structure collected from Rietveld refinement are described in Table 1.

Table 1

Crystallographic data at room temperature for SBSC. Cell parameters were collected using a Rietveld refinement

Atom	Wyckoff position	x	y	z	Uiso	Occ
Sm	1a (0 0 0)	0	0	0	0.0333	0.8797
Co	2h (½ ½ z)	1/2	1/2	0.25592	0.0045	0.9944
Ba/Sr	1b (0 0 ½)	0	0	1/2	0.0092	0.8926
O1	4i (0 ½ z)	0	1/2	0.26780	0.0077	0.9311
O2	1c (½ ½ 0)	1/2	1/2	0	0.1906	1.2455
O3	2h (½ ½ z)	1/2	1/2	0.44110	0.0333	0.4220

Meanwhile, the Co atom occupies position 2h (0.5, 0.5, z). The SBSC structure has three kinds of oxygen atom sites: O3 at 2h (0.5, 0.5, z), O2 at 1c (0.5, 0.5, 0), and O1 at 4i (0, 0.5, z).

Fig. 3 shows the refinement of SBSC patterns, including the measured XRD data, the calculated profile, and the difference between them. The refinement using the General Structure Analysis System (GSAS) program is typically used for crystallographic analysis, quantitative phase determination, texture mapping, stress-strain measurements, and other related types of materials characterization. The test results agree with the measured profiles, indicating that in the perovskite lattice, cations are well ordered.

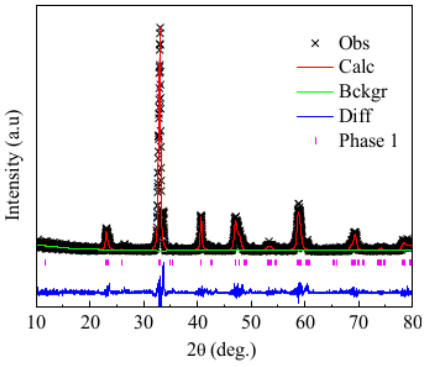

Fig. 3. Rietveld refinement data of the SBSC cathode at room temperature

The space group, fractional coordinates, and lattice parameters of corresponding double perovskite structure cathodes are shown in Table 2.

Table 2

Space group, fractional coordinates, and lattice parameters of corresponding double perovskite structure cathodes

Specimens	Space group	a(⊕)	b(⊕)	c(⊕)	V(⊕)	R_{wp}
$NdBaCo_2O_{5+\delta}$ [29]	P4/mmm	3.903	3.903	7.614	116.02	0.42
$SmBaCoO_{5+\delta}$ [29]	Pmmm	3.886	7.833	7.560	230.22	0.45
$NdBa_{0.5}Sr_{0.5}Co_2O_{5+\delta}$ [30]	P4/mmm	3.861	3.861	7.715	115.01	0.36
$NdBa_{0.5}Sr0.5Co_{1.5}Mn_{0.5}O_{5+\delta}$ [31]	P4/mmm	3.855	3.855	7.705	114.54	0.12
$SmBa_{0.6}Sr_{0.4}Co_2O_{5+\delta}$ [11]	P4/mmm	3.870	3.870	7.590	114.11	0.29
$SmBa_{0.5}Sr_{0.5}Co_2O_{5+\delta}$ [32]	P4/mmm	3.883	3.883	7.580	114.30	0.28

The SBSC cathode showed high structural stability when the samples were calcined under temperatures of 1,000 °C and 1,200 °C, which does not influence the crystal structure [33].

5. 2. Thermal properties and oxygen content analysis

To clarify the oxygen content of the SBSC cathode, TGA was conducted in the air. The TGA curve indicates that the specimen had a slight weight loss before 125 °C, which is associated with the desorption of the specimen's absorbed water as presented in Fig. 4, *a*. With a further increase in temperature, the magnitude of weight loss became significant and continued until weight loss slowed at temperatures of 250–325 °C.

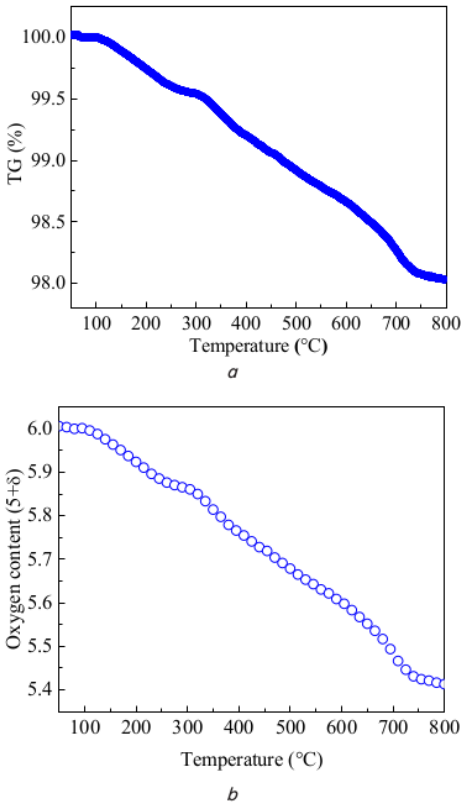

Fig. 4. Curve data: *a* — TGA of the SBSC powder over a temperature range between 27 °C and 800 °C; *b* — oxygen content (5+δ) as a function of temperature in air for SBSC cathodes

Above 325 °C, the rate of degradation in weight loss was significant, and the mass change slowed again at temperatures around 725 °C. It can be seen that from 650 °C to 750 °C the weight loss rate tends to increase. Then, at a temperature range of 750 °C, weight loss seems to slow down again until it reaches a temperature of 800 °C. Detailed oxygen content (5+δ) information as a function of temperature is listed in Table 3.

Table 3

5+δ as a function of temperature in air for the SBSC cathode

Specimens	Calcination temperature (°C)	5+δ			
		200 °C	400 °C	600 °C	800 °C
SBSC91 [25]	1,200	5.53	5.44	5.32	5.18
SBSC73 [25]	1,200	5.62	5.55	5.36	5.22
SBSC55 [25]	1,200	5.74	5.64	5.51	5.39
SBSC [this work]	1,000	5.92	5.76	5.60	5.41

The calcination temperature has an impact on the oxygen content of the SBSC cathode. The oxygen content of the cathode with a calcination temperature of 1200 °C is smaller than that of a calcined one at a temperature of 1,000 °C. In the cathode with the calcination temperature of 1,200 °C, the oxygen content values were 5.74 (200 °C) and 5.39 (800 °C), while in the cathode with the calcination temperature of 1,000 °C, the oxygen content values obtained were 5.92 and 5.41.

5. 3. OPP Half-Cell

Typical impedance spectra for symmetrical cells (SBSC|SDC|SBSC) were obtained by AC impedance spectroscopy. Fig. 5 shows the fitting data of impedance spectra for symmetrical cells measured at different temperatures such as *a* – 600 °C; *b* –700 °C; and *c* – 800 °C, serially. While the various OPPs were employed from 0.214–0.035 atm. The polarization resistance (R_p) was a function of $p(O_2)$, which is investigated under various temperatures between 600 °C to 800 °C with the OPPs ranged from 0.214 to 0.035 atm.

The R_p values increased with decreasing $p(O_2)$ values due to the decrease in mobile interstitial oxygen at lower $p(O_2)$ values. The fitting of the impedance spectrum for symmetrical cells using the Z-View program.

The R_p value of the specimen was significantly reduced at 800 °C with an oxygen **partial pressure** (OPP) of 0.214 atm as presented in Fig. 6.

Table 4

Interfacial polarization resistance (R_p) as a function of $p(O_2)$ for SBSC|SDC|SBSC symmetrical cells

$p(O_2)$ (atm)	R_p (Ωcm^2)		
	600 °C	700 °C	800 °C
0.214	4.02	1.04	0.42
0.112	4.62	1.06	0.43
0.074	4.90	1.08	0.45
0.050	5.10	1.10	0.47
0.035	5.32	1.20	0.49

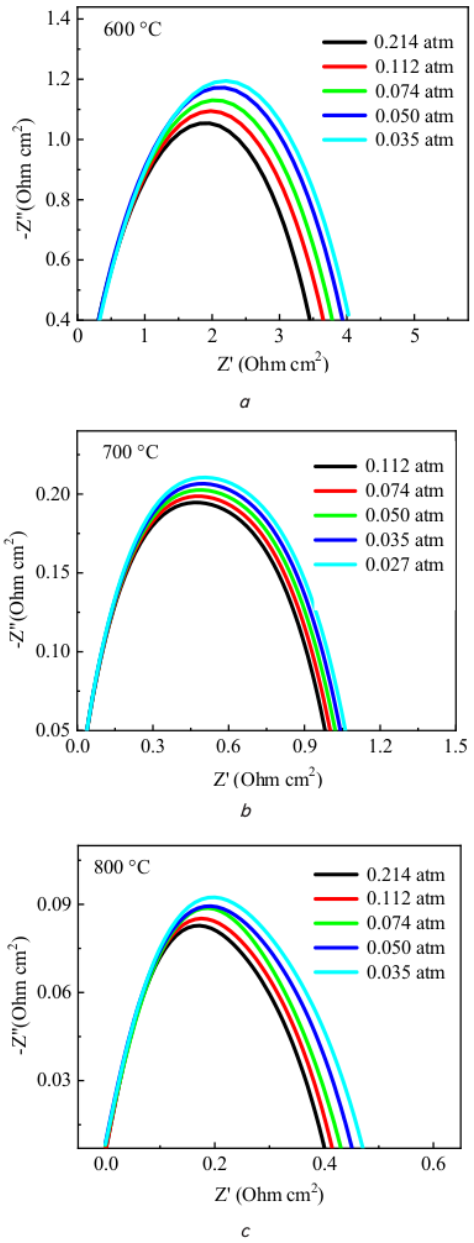

Fig. 5. Fitting data of impedance spectra for symmetrical cells measured at: *a* – 600 °C; *b* –700 °C; *c* – 800 °C. Various OPPs from 0.214–0.035 atm

The cathode cell performance is influenced by the R_p values obtained from the components. The high R_p values have a significant impact on SOFC performance. In general, the value of R_p has decreased with the increase in the working temperature of the SOFC. In these conditions, the manufacture of SOFC components, especially the high density between layers (anode, electrolyte, and cathode), is of great concern to researchers.

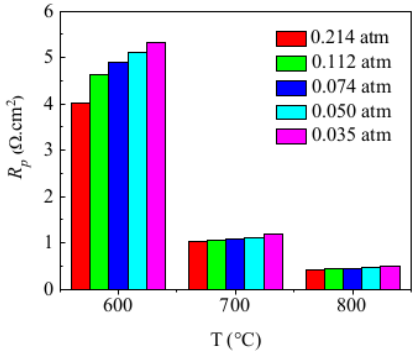

Fig. 6. Interfacial polarization resistance (R_p) as a function of $p(O_2)$ for SBSC|SDC|SBSC symmetrical cells at 600 °C, 700 °C, and 800 °C

5. 4. Single-Cell Performance

Fig. 7 shows the single-cell performance of anode-supported Ni-SDC|SDC|SBSC under air/humidified hydrogen (3 vol % H_2O). Increasing temperature has an impact on increasing the current density and power density due to the thermally activated kinetic process [34]. Due to the same phenomenon, cell voltage increased at higher temperatures. Fig. 4 also indicates that the open-circuit voltages (OCVs) are 0.83, 0.81, and 0.84 at 425 °C, 450 °C, and 475 °C, respectively; these values are lower than the theoretical values.

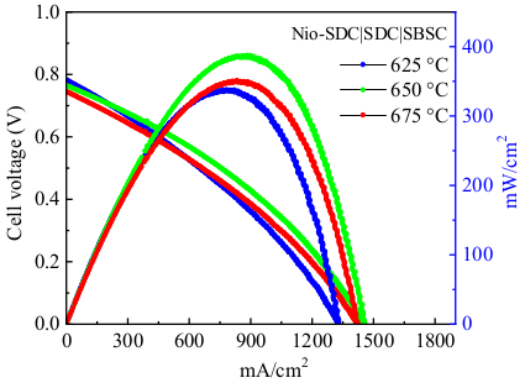

Fig. 7. Performance of a single cell of Ni-SDC|SDC|SBSC at temperatures ranging from 625 °C to 675 °C

The cathode performance in the SOFC cell is shown in Fig. 6, the power density at 650 °C exceeds that of the cell at 675 °C. This phenomenon needs to be analyzed more deeply because in general, the performance of SOFC cells increases with an increased operating temperature range between 600 °C and 800 °C. With these results, it can be stated that the SBSC oxide works well as a SOFC cathode at intermediate operating temperature.

5. 5. SEM Image

Fig. 8 displays the SEM images of *a* – cross-sectional image of the SBSC cathode in the SBSC|SDC|SBSC symmetrical-cell specimen and *b* – top view of the SBSC cathode. In the symmetric cell, the cathode layer of SBSC was calcined in air for 2 h at 1,000 °C. A uniform porous microstructure facilitates the gas diffusion of the cathode layer. A well-connected electrolyte–cathode interface determines low resistance in the solid oxide fuel cell.

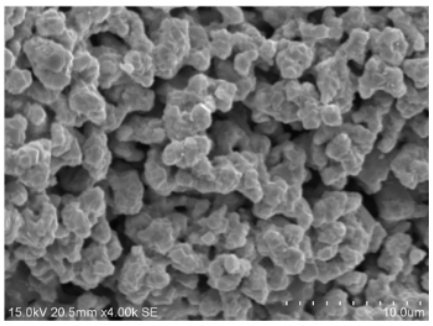

a

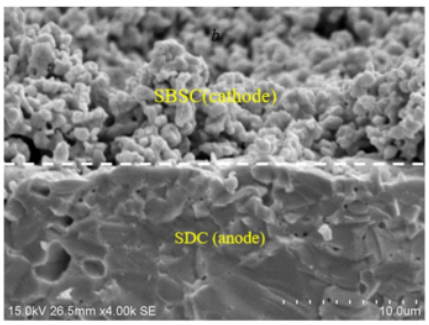

b

Fig. 8. SEM image: *a* – cross-sectional SEM image of the SBSC cathode in the SBSC|SDC|SBSC symmetrical cell specimen prepared at 1,000 °C for 2 h; *b* – top view of the SBSC cathode

In Fig. 8, *b*, the adhesion between the SDC electrolyte and the SBSC cathode layer is quite good. Fig. 8, *b* consists of two layers covering the SBCC (cathode) on the top and SDC (anode) on the bottom. The white line shows the two-layer boundary between the cathode and anode. The SBSC cathode grain size is distributed uniformly in the range of 1.5–2 μm and is porous.

6. Discussion of experimental results

The XRD pattern of SBSC powder, which can be categorized into a tetragonal space group (P4/mmm) is as shown in Fig. 3, after calcining at 1,000 °C for 6 h. There is a good compatibility level between the experimental data and calculated profiles, which shows that the cations are ordered well in the perovskite lattice arrangement between the Sm^{3+} and Ba^{2+}/Sr^{2+} ions [35].

The overall change in mass of the SBSC powder reached 8 % at temperatures of 125–800 °C. Previous data showed that the specimen was beginning to lose lattice oxygen significantly at a specific temperature [36]. Lattice oxygen is concerned with the reduction and oxidation of perovskite

oxides. The oxygen void is experienced by perovskite oxide when lattice oxygen is released. A partial loss of lattice oxygen, along with a reduction in Co^{3+} to Co^{2+}, or Co^{4+} to Co^{3+}, and an increase in temperature, causes a decrease in weight loss during heating. Therefore, the oxygen content decreases with temperature [37, 38]. The high diffusivity regarding oxide ions and the increased surface activity of the ORRs might be due to a high oxygen content [39].

To clarify the polarization of the SBSC cathode resistance, the symmetrical cells test was carried out with various OPPs from 0.214–0.035 atm. From the data, with increasing temperatures, the R_p values fell dramatically, suggesting that the SBSC sample ORR is a thermally activated process. The R_p values of the specimen reduced from 4.02 Ωcm^2 at 600 °C to 0.42 Ωcm^2 at 800 °C with an OPP of 0.214 atm as presented in Fig. 6. However, the R_p values increased significantly with a decreasing oxygen partial pressure. For instance, as $p(O_2)$ decreases from 0.214 to 0.035 atm, the R_p value increases from 4.02 to 5.32 Ωcm^2 at a temperature of 600 °C. This study is consistent with the results previously reported by Meng et al. regarding changes in polarization resistance to oxygen partial pressure [40]. The R_p values reflect cathodic behavior, including diffusion of oxygen at high temperatures in the gas phase, low-temperature ORR, and the surface of bulk diffusion/oxygen [41].

From single cell testing, ideally, the OCV of a cell should be similar to its 1.1 V theoretical value and should be small only if affected by factors of operating conditions. Porosity impacts the leakage current when fuel/oxidants crossing the electrolyte membrane can cause low OCV values. The following equation can explain the concept of chemical defect:

$$Ce_{Ce} \rightarrow Ce'_{Ce} + h. \quad (5)$$

Electrolyte-based materials with low electronic conductivity, such as SDC, may lead to a slight electron cross flow via the electrolyte. Alternatively, Ce^{4+} in SDC electrolytes is quickly reduced to Ce^{3+}, particularly at higher temperatures [29]. The power density values of the cell with an SBSC cathode are 336.1, 387.3, and 357.4 mW/cm^2 at 625 °C, 650 °C, and 675 °C, respectively. One method of improving cell performance is by modifying the cathode surface using electrolyte-based materials such as SDC. As previously reported, SDC nanoparticles implanted into the porous surface of the cathode produce a significant increase in the power density value [42].

Fig. 8 shows a cross-sectional view of SBSC|SDC from the prepared symmetrical cell and top surface SEM images. The SBSC cathode grain size is distributed uniformly in the range of 1.5–2 μm and is porous. Better morphology is very helpful to ensure increased current, reduced R_p values, and rapid oxygen diffusion during SOFC operations. Also, the cathode structure's properties determine the cell performance in processes such as kinetic reactions, mass transportation preprocesses, and charge transportation [43].

Overall, we have presented the SBSC perovskite oxide investigation in this report. However, a more comprehensive study is needed to improve SOFC performance, including thermal expansion testing to determine the degradation resistance between SOFC layers. In the future work, we will focus on increasing the value of open-circuit voltage (OCV) using a dense bi-layer electrolyte of Yttria-stabilized Zirconia (YSZ)/Samaria doped Ceria (SDC) through pulsed laser deposition (PLD) technique. YSZ dense layer prepared by pulsed laser deposition (PLD) technique as a blocking layer improved the stability of the SDC electrolyte and inhibited electronic current leakage. This method is expected to increase the value of OCV and the single-cell performance.

7. Conclusions

1. The XRD structure of the SBSC cathode has been successfully categorized as double perovskite oxide by the solid-state reaction method. The double perovskite structure consists of the elements Sm^{3+}, Ba^{2+} on the A side and Sr^{2+}, Co^{3+} on the B side.

2. The R_p values of the specimen decreased from 4.02 Ωcm^2 at 600 °C to 0.42 Ωcm^2 at 800 °C. The maximum power density of the single cell is 387.3 mW/cm^2 at 650 °C, indicating that SBSC is qualified as the SOFC cathode material.

3. SBSC cathodes show good performance at intermediate operating temperatures (600–800 °C).

Acknowledgments

The authors are grateful for the financial support provided by the Institut Teknologi Nasional Yogyakarta (Indonesia). The authors are also grateful for the financial support by A113 Laboratory of MSE (NDHU) and grand funded through MOST 106-2113-M-259-011 by the Ministry of Science and Technology of Taiwan.

References

1. Steele, B. C. H., Heinzel, A. (2001). Materials for fuel-cell technologies. Nature, 414 (6861), 345–352. doi: https://doi.org/10.1038/35104620
2. Minh, N. Q. (1993). Ceramic Fuel Cells. Journal of the American Ceramic Society, 76 (3), 563–588. doi: https://doi.org/10.1111/j.1151-2916.1993.tb03645.x
3. Ruiz-Morales, J. C., Marrero-López, D., Canales-Vázquez, J., Irvine, J. T. S. (2011). Symmetric and reversible solid oxide fuel cells. RSC Advances, 1 (8), 1403. doi: https://doi.org/10.1039/c1ra00284h
4. Skinner, S. J. (2001). Recent advances in Perovskite-type materials for solid oxide fuel cell cathodes. International Journal of Inorganic Materials, 3 (2), 113–121. doi: https://doi.org/10.1016/s1466-6049(01)00004-6
5. Brett, D. J. L., Atkinson, A., Brandon, N. P., Skinner, S. J. (2008). Intermediate temperature solid oxide fuel cells. Chemical Society Reviews, 37 (8), 1568. doi: https://doi.org/10.1039/b612060c
6. Susanto, I., Kamal, D. M., Ruswanto, S., Subarkah, R., Zainuri, F., Permana, S. et. al. (2020). Development of cobalt-free oxide ($Sm_{0.5}Sr_{0.5}Fe_{0.8}Cr0._2O_{3-\delta}$) cathode for intermediate-temperature solid oxide fuel cells (IT-SOFCs). Eastern-European Journal of Enterprise Technologies, 6 (5 (108)), 15–20. doi: https://doi.org/10.15587/1729-4061.2020.217282

7. Liu, H., Zhu, X., Cheng, M., Cong, Y., Yang, W. (2011). Novel Mn1.5Co1.5O4spinel cathodes for intermediate temperature solid oxidefuel cells. Chemical Communications, 47 (8), 2378–2380. doi: https://doi.org/10.1039/c0cc04300a
8. Adler, S. B. (2004). Factors Governing Oxygen Reduction in Solid Oxide Fuel Cell Cathodes†. Chemical Reviews, 104 (10), 4791–4844. doi: https://doi.org/10.1021/cr020724o
9. Takeda, Y., Kanno, R., Noda, M., Tomida, Y., Yamamoto, O. (1987). Cathodic Polarization Phenomena of Perovskite Oxide Electrodes with Stabilized Zirconia. Journal of The Electrochemical Society, 134 (11), 2656–2661. doi: https://doi.org/10.1149/1.2100267
10. Adler, S. B., Lane, J. A., Steele, B. C. H. (1996). Electrode Kinetics of Porous Mixed-Conducting Oxygen Electrodes. Journal of The Electrochemical Society, 143 (11), 3554–3564. doi: https://doi.org/10.1149/1.1837252
11. Subardi, A., Cheng, M.-H., Fu, Y.-P. (2014). Chemical bulk diffusion and electrochemical properties of $SmBa_{0.6}Sr_{0.4}Co_2O_5$+ cathode for intermediate solid oxide fuel cells. International Journal of Hydrogen Energy, 39 (35), 20783–20790. doi: https://doi.org/10.1016/j.ijhydene.2014.06.134
12. Zhao, F., Wang, S., Brinkman, K., Chen, F. (2010). Layered perovskite $PrBa_{0.5}Sr_{0.5}Co_2O_{5+\delta}$ as high performance cathode for solid oxide fuel cells using oxide proton-conducting electrolyte. Journal of Power Sources, 195 (17), 5468–5473. doi: https://doi.org/10.1016/j.jpowsour.2010.03.088
13. Zhou, Q., He, T., Ji, Y. (2008). $SmBaCo_2O_{5+x}$ double-perovskite structure cathode material for intermediate-temperature solid-oxide fuel cells. Journal of Power Sources, 185 (2), 754–758. doi: https://doi.org/10.1016/j.jpowsour.2008.07.064
14. Tarancón, A., Burriel, M., Santiso, J., Skinner, S. J., Kilner, J. A. (2010). Advances in layered oxide cathodes for intermediate temperature solid oxide fuel cells. Journal of Materials Chemistry, 20 (19), 3799. doi: https://doi.org/10.1039/b922430k
15. Chen, D., Ran, R., Zhang, K., Wang, J., Shao, Z. (2009). Intermediate-temperature electrochemical performance of a polycrystalline $PrBaCo_2O_{5+\delta}$ cathode on samarium-doped ceria electrolyte. Journal of Power Sources, 188 (1), 96–105. doi: https://doi.org/10.1016/j.jpowsour.2008.11.045
16. Kuroda, C., Zheng, K., Świerczek, K. (2013). Characterization of novel $GdBa_{0.5}Sr_{0.5}Co_2$–$xFexO_{5+\delta}$ perovskites for application in IT-SOFC cells. International Journal of Hydrogen Energy, 38 (2), 1027–1038. doi: https://doi.org/10.1016/j.ijhydene.2012.10.085
17. Tarancón, A., Morata, A., Dezanneau, G., Skinner, S. J., Kilner, J. A., Estradé, S. et. al. (2007). GdBaCo2O5+x layered perovskite as an intermediate temperature solid oxide fuel cell cathode. Journal of Power Sources, 174 (1), 255–263. doi: https://doi.org/10.1016/j.jpowsour.2007.08.077
18. Chang, A., Skinner, S., Kilner, J. (2006). Electrical properties of $GdBaCo_2O_{5+x}$ for ITSOFC applications. Solid State Ionics, 177 (19-25), 2009–2011. doi: https://doi.org/10.1016/j.ssi.2006.05.047
19. Gu, H., Chen, H., Gao, L., Zheng, Y., Zhu, X., Guo, L. (2009). Oxygen reduction mechanism of $NdBaCo_2O_{5+\delta}$ cathode for intermediate-temperature solid oxide fuel cells under cathodic polarization. International Journal of Hydrogen Energy, 34 (5), 2416–2420. doi: https://doi.org/10.1016/j.ijhydene.2009.01.003
20. Kong, X., Ding, X. (2011). Novel layered perovskite $SmBaCu_2O_{5+\delta}$ as a potential cathode for intermediate temperature solid oxide fuel cells. International Journal of Hydrogen Energy, 36 (24), 15715–15721. doi: https://doi.org/10.1016/j.ijhydene.2011.09.035
21. Kim, J. H., Kim, Y., Connor, P. A., Irvine, J. T. S., Bae, J., Zhou, W. (2009). Structural, thermal and electrochemical properties of layered perovskite $SmBaCo_2O_{5+d}$, a potential cathode material for intermediate-temperature solid oxide fuel cells. Journal of Power Sources, 194 (2), 704–711. doi: https://doi.org/10.1016/j.jpowsour.2009.06.024
22. Liu, W., Yang, C., Wu, X., Gao, H., Chen, Z. (2011). Oxygen relaxation and phase transition in $GdBaCo_2O_{5+\delta}$ oxide. Solid State Ionics, 192 (1), 245–247. doi: https://doi.org/10.1016/j.ssi.2010.04.028
23. Kim, J.-H., Mogni, L., Prado, F., Caneiro, A., Alonso, J. A., Manthiram, A. (2009). High Temperature Crystal Chemistry and Oxygen Permeation Properties of the Mixed Ionic–Electronic Conductors $LnBaCo_2O_{5+\delta}$ (Ln = Lanthanide). Journal of The Electrochemical Society, 156 (12), B1376. doi: https://doi.org/10.1149/1.3231501
24. Subardi, A., Chen, C.-C., Cheng, M.-H., Chang, W.-K., Fu, Y.-P. (2016). Electrical, thermal and electrochemical properties of $SmBa1–xSrxCo_2O_{5+\delta}$ cathode materials for intermediate-temperature solid oxide fuel cells. Electrochimica Acta, 204, 118–127. doi: https://doi.org/10.1016/j.electacta.2016.04.069
25. Lü, S., Long, G., Meng, X., Ji, Y., Lü, B., Zhao, H. (2012). $PrBa_{0.5}Sr_{0.5}Co_2O_{5+x}$ as cathode material based on LSGM and GDC electrolyte for intermediate-temperature solid oxide fuel cells. International Journal of Hydrogen Energy, 37 (7), 5914–5919. doi: https://doi.org/10.1016/j.ijhydene.2011.12.134
26. Fu, Y.-P., Wen, S.-B., Lu, C.-H. (2007). Preparation and Characterization of Samaria-Doped Ceria Electrolyte Materials for Solid Oxide Fuel Cells. Journal of the American Ceramic Society, 91 (1), 127–131. doi: https://doi.org/10.1111/j.1551-2916.2007.01923.x
27. Kuhn, M., Kim, J. J., Bishop, S. R., Tuller, H. L. (2013). Oxygen Nonstoichiometry and Defect Chemistry of Perovskite-Structured $BaxSr1–xTi1–yFeyO_{3–y/2+\delta}$ Solid Solutions. Chemistry of Materials, 25 (15), 2970–2975. doi: https://doi.org/10.1021/cm400546z
28. Fu, Y.-P., Ouyang, J., Li, C.-H., Hu, S.-H. (2013). Chemical bulk diffusion coefficient of $Sm_{0.5}Sr_{0.5}CoO_{3-\delta}$ cathode for solid oxide fuel cells. Journal of Power Sources, 240, 168–177. doi: https://doi.org/10.1016/j.jpowsour.2013.03.138
29. Aksenova, T. V., Gavrilova, L. Y., Yaremchenko, A. A., Cherepanov, V. A., Kharton, V. V. (2010). Oxygen nonstoichiometry, thermal expansion and high-temperature electrical properties of layered $NdBaCo_2O_{5+\delta}$ and $SmBaCo_2O_{5+\delta}$. Materials Research Bulletin, 45 (9), 1288–1292. doi: https://doi.org/10.1016/j.materresbull.2010.05.004

30. Zhang, K., Ge, L., Ran, R., Shao, Z., Liu, S. (2008). Synthesis, characterization and evaluation of cation-ordered $LnBaCo_2O_{5+\delta}$ as materials of oxygen permeation membranes and cathodes of SOFCs. Acta Materialia, 56 (17), 4876–4889. doi: https://doi.org/10.1016/j.actamat.2008.06.004
31. Kim, J., Choi, S., Park, S., Kim, C., Shin, J., Kim, G. (2013). Effect of Mn on the electrochemical properties of a layered perovskite $NdBa_{0.5}Sr_{0.5}Co_{2-x}MnxO_{5+\delta}$ (x=0, 0.25, and 0.5) for intermediate-temperature solid oxide fuel cells. Electrochimica Acta, 112, 712–718. doi: https://doi.org/10.1016/j.electacta.2013.09.014
32. Subardi, A., Fu, Y.-P. (2017). Electrochemical and thermal properties of $SmBa_{0.5}Sr_{0.5}Co_2O_{5+\delta}$ cathode impregnated with $Ce_{0.8}Sm_{0.2}O1.9$ nanoparticles for intermediate-temperature solid oxide fuel cells. International Journal of Hydrogen Energy, 42 (38), 24338–24346. doi: https://doi.org/10.1016/j.ijhydene.2017.08.010
33. West, M., Manthiram, A. (2013). Layered $LnBa1-xSrxCoCuO_{5+\delta}$ (Ln = Nd and Gd) perovskite cathodes for intermediate temperature solid oxide fuel cells. International Journal of Hydrogen Energy, 38 (8), 3364–3372. doi: https://doi.org/10.1016/j.ijhydene.2012.12.133
34. Choi, M.-B., Lee, K.-T., Yoon, H.-S., Jeon, S.-Y., Wachsman, E. D., Song, S.-J. (2012). Electrochemical properties of ceria-based intermediate temperature solid oxide fuel cell using microwave heat-treated $La_{0.1}Sr_{0.9}Co_{0.8}Fe_{0.2}O_{3-\delta}$ as a cathode. Journal of Power Sources, 220, 377–382. doi: https://doi.org/10.1016/j.jpowsour.2012.07.122
35. Jun, A., Shin, J., Kim, G. (2013). High redox and performance stability of layered $SmBa_{0.5}Sr_{0.5}Co_{1.5}Cu_{0.5}O_{5+\delta}$ perovskite cathodes for intermediate-temperature solid oxide fuel cells. Physical Chemistry Chemical Physics, 15 (45), 19906. doi: https://doi.org/10.1039/c3cp53883d
36. Kostogloudis, G., Vasilakos, N., Ftikos, Ch. (1998). Crystal structure, thermal and electrical properties of $Pr1-xSrxCoO_{3-\delta}$ (x=0, 0.15, 0.3, 0.4, 0.5) perovskite oxides. Solid State Ionics, 106 (3-4), 207–218. doi: https://doi.org/10.1016/s0167-2738(97)00506-7
37. Meuffels, P. (2007). Propane gas sensing with high-density $SrTi_{0.6}Fe_{0.4}O_{(3-\delta)}$ ceramics evaluated by thermogravimetric analysis. Journal of the European Ceramic Society, 27 (1), 285–290. doi: https://doi.org/10.1016/j.jeurceramsoc.2006.05.078
38. Lia, S., Jin, W., Xu, N., Shi, J. (2001). Mechanical strength, and oxygen and electronic transport properties of $SrCo_{0.4}Fe_{0.6}O_{3-\delta}$-YSZ membranes. Journal of Membrane Science, 186 (2), 195–204. doi: https://doi.org/10.1016/s0376-7388(00)00681-5
39. Kim, G., Wang, S., Jacobson, A. J., Reimus, L., Brodersen, P., & Mims, C. A. (2007). Rapid oxygen ion diffusion and surface exchange kinetics in $PrBaCo_2O_{5+x}$ with a perovskite related structure and ordered A cations. Journal of Materials Chemistry, 17 (24), 2500. doi: https://doi.org/10.1039/b618345j
40. Meng, F., Xia, T., Wang, J., Shi, Z., Lian, J., Zhao, H. et. al. (2014). Evaluation of layered perovskites $YBa1-xSrxCo_2O_{5+\delta}$ as cathodes for intermediate-temperature solid oxide fuel cells. International Journal of Hydrogen Energy, 39 (9), 4531–4543. doi: https://doi.org/10.1016/j.ijhydene.2014.01.008
41. Baek, S.-W., Kim, J. H., Bae, J. (2008). Characteristics of ABO_3 and A_2BO_4 (ASm, Sr; BCo, Fe, Ni) samarium oxide system as cathode materials for intermediate temperature-operating solid oxide fuel cell. Solid State Ionics, 179 (27-32), 1570–1574. doi: https://doi.org/10.1016/j.ssi.2007.12.010
42. Nam, J. H., Jeon, D. H. (2006). A comprehensive micro-scale model for transport and reaction in intermediate temperature solid oxide fuel cells. Electrochimica Acta, 51 (17), 3446–3460. doi: https://doi.org/10.1016/j.electacta.2005.09.041
43. Andersson, M., Yuan, J., Sundén, B. (2010). Review on modeling development for multiscale chemical reactions coupled transport phenomena in solid oxide fuel cells. Applied Energy, 87 (5), 1461–1476. doi: https://doi.org/10.1016/j.apenergy.2009.11.013

AN ANALYSIS OF SmBa 0.5Sr UDC 539 0.5CO2O5+δ DOUBLE PEROVSKITE OXIDE FOR INTERMEDIATE–EMPERATURE SOLID OXIDE FUEL CELLS

ORIGINALITY REPORT

19%
SIMILARITY INDEX

MATCH ALL SOURCES (ONLY SELECTED SOURCE PRINTED)

★Adi Subardi, Yen-Pei Fu. "Electrochemical and thermal properties of SmBa0.5Sr0.5Co2O5+δ cathode impregnated with Ce0.8Sm0.2O1.9 nanoparticles for intermediate-temperature solid oxide fuel cells", International Journal of Hydrogen Energy, 2017 3%
Crossref

EXCLUDE QUOTES ON
EXCLUDE BIBLIOGRAPHY ON
EXCLUDE MATCHES OFF